

A Model for the 19th Century Eruption of Eta Carinae: CSM Interaction Like a Scaled-Down Type IIn Supernova

Nathan Smith*

Steward Observatory, University of Arizona, 933 North Cherry Avenue, Tucson, AZ 85721, USA

Accepted 0000, Received 0000, in original form 0000

ABSTRACT

This paper proposes a simple model for the 19th century eruption of Eta Carinae that consists of two components: (1) a strong wind ($\dot{M} = 0.33 M_{\odot} \text{ yr}^{-1}$; $v_{\infty} = 200 \text{ km s}^{-1}$), blowing for 30 years, followed by (2) a $\sim 10^{50}$ erg explosion ($10 M_{\odot}$; $750\text{--}1000 \text{ km s}^{-1}$) occurring in 1844. The ensuing collision between the fast ejecta and the dense circumstellar material (CSM) causes an increase in brightness observed at the end of 1844, followed by a sustained high-luminosity phase lasting for 10–15 years that provides a close match to the observed historical light curve. The emergent luminosity is powered by converting kinetic energy to radiation through CSM interaction, analogous to the process occurring in more luminous Type IIn supernovae, except with ~ 10 times lower explosion energy and at slower speeds (causing a longer duration and lower emergent luminosity). We demonstrate that such an explosive event not only provides a natural explanation for the light curve evolution, but also accounts for a number of puzzling attributes of the highly scrutinized Homunculus, including: (1) rough equipartition of total radiated and kinetic energy in the event, (2) the double-shell structure of the Homunculus, with a thin massive outer shell (corresponding to the coasting cold dense shell) and a thicker inner layer (between the cold dense shell and the reverse shock), (3) the apparent single age and Hubble-like flow of the Homunculus resulting from the thin swept-up shell, (4) the complex mottled appearance of the polar lobes in *Hubble Space Telescope* images, arising naturally from Raleigh-Taylor or Vishniac instabilities at the contact discontinuity of the shock, (5) efficient and rapid dust formation, which has been observed in the post-shock zones of Type IIn supernovae, and (6) the fast ($3000\text{--}5000 \text{ km s}^{-1}$) material outside the Homunculus, arising from the acceleration of the forward shock upon exiting the dense CSM. In principle, the bipolar shape has already been explained following earlier studies of interacting winds, except that here the requisite pre-existing “torus” may be provided by periastron collisions occurring around the same time, and the CSM interaction occurs over only 10 years, producing a thin shell with the resulting structures then frozen-in to a homologously expanding bipolar nebula. This self-consistent picture has a number of implications for other eruptive transients, many of which may also be powered by CSM interaction. A key remaining unknown is the ultimate source of the 10^{50} ergs of energy required in the explosion.

Key words: circumstellar matter — instabilities — stars: evolution — stars: individual (Eta Carinae) — stars: mass loss — stars: winds, outflows

1 INTRODUCTION

The chief reason why η Carinae is an object of perpetual astrophysical mystery is that the cause of its so-called “Great Eruption” in the mid-19th century remains unexplained. During this event (see Davidson & Humphreys

1997; Humphreys et al. 1999; Smith & Frew 2011), the star increased its bolometric luminosity and is thought to have exceeded the classical Eddington limit by a factor of roughly 5 as it briefly became the second brightest star in the night sky, despite its distance of ~ 2.3 kpc (Smith 2006). During this event, the star also created the bipolar Homunculus nebula, which has been studied in exquisite detail with the *Hubble Space Telescope* (*HST*) and numerous

* Email: nathans@as.arizona.edu

other observatories. The total radiated energy of the eruption ($\int L dt = 10^{49.3}$ ergs; Smith et al. 2011; Humphreys et al. 1999) and the kinetic energy of the expanding Homunculus nebula (about $10^{49.7}$ ergs; Smith et al. 2003b) released by this eruption rivaled that of a normal supernova (SN), but the star survived the event — and there are clues from its extensive nebulosity that it may have done this multiple times in the past (e.g., Walborn 1976; Smith & Morse 2004).

This eruption has been adopted as the prototype for a class of stellar outbursts, a number of which have now been identified in other galaxies (see Van Dyk 2005; Van Dyk & Matheson 2012; Smith et al. 2011). These extragalactic η Car analogs masquerade as Type II_n supernovae (SNe II_n), and are sometimes called “supernova impostors” due to their regular discovery in SN searches. This type of outburst may be a common — although very brief — rite of passage in the evolution of very massive stars, and could dominate the total mass lost by a massive star during its lifetime (Smith & Owocki 2006; Kochanek 2011). Furthermore, the mass loss mechanism may be nearly independent of metallicity, and therefore may offer a mode of mass loss even for metal-poor massive stars in the early universe (Smith & Owocki 2006; van Marle et al. 2008). Eruptive mass-loss akin to the Great Eruption of η Car is also thought to occur within a few years to decades before some of the most luminous SNe II_n known (e.g., Smith et al. 2007, 2010a; Smith & McCray 2007; Ofek et al. 2007; Woosley et al. 2007; Chevalier & Irwin 2011). The underlying instability that causes these events, however, remains unproven and presents a fundamental roadblock in our understanding of stellar evolution for massive stars in general, and Population III stars in particular.

Recent observations imply that most of the mass or energy ejection in the 19th century outburst of η Carinae occurred over a very short time. The most telling are the extremely thin and dense walls of the Homunculus nebula (Smith 2006) and the small dispersion in ejection dates derived from its expansion (Morse et al. 2001). These imply that the main ejection phase lasted only about 5 yr or less. Combined with the large amount of mass contained in the thin walls of the polar lobes of the Homunculus (more than $10 M_{\odot}$; Smith et al. 2003), this would require a mass-loss rate during the eruption in excess of a few $M_{\odot} \text{ yr}^{-1}$. Such enormous mass flux is well beyond the capability of a line-driven wind (Castor et al. 1975; Aerts et al. 2004), and may even exceed the capability of a super-Eddington continuum-driven wind alone (Owocki, Gayley, & Shaviv 2004). The ratio of mechanical to radiated energy is well over unity (roughly a factor of 3; see above), implying that the 19th century event was more like an explosion than a normal radiation-driven wind (Smith et al. 2003). Very high speeds observed in the surrounding CSM outside the Homunculus also seem to imply an explosive component in the event, which is harder to explain in any wind scenario alone (Smith 2008). Moreover, reanalysis of the historical light curve shows brief brightening events associated with times of periastron (Smith & Frew 2011) and the recent discovery of light echoes from the Great Eruption and associated spectra challenge the conventional interpretation of a wind-driven event (Rest et al. 2012).

Following the hypothesis that the Great Eruption was powered by an explosive event rather than a steady wind, this paper explores potential consequences for understand-

ing the historical light curve of η Car (Smith & Frew 2011) and the formation of various structures in the complex Homunculus nebula. This paper treats the event as an explosion to see if it provides a viable explanation for the observed light curve. In this context, such an explosion must be non-terminal so that the star’s core remains in-tact, as the star is still observed to be luminous at the present time.

The most significant consequence of assuming an explosive origin for the event is that radiation from the conversion of ejecta kinetic energy into radiation can circumvent the paradox of exceeding the classical Eddington limit for 20 years (much longer than the dynamical time), because the radiating atmosphere is no longer required to be hydrostatic. It can also help explain how η Car was able to drastically change its radiative luminosity much faster than a thermal timescale during the brief precursor brightening events in 1843 and 1838 (Smith & Frew 2011; Smith 2011).

The model suggested below invokes an unknown physical mechanism to cause an explosion that suddenly injected a large amount of kinetic energy. Although there exists no firmly-established theoretical basis for this, it is supported by a number of observational consequences. As shown below, an explosion that overtakes a previously existing dense wind can provide a natural explanation for both the emergent luminosity of the event and its evolution with time, as well as several detailed physical and structural properties of the Homunculus nebula. A simple CSM interaction model is presented in §2. In §3 we then discuss how we can explain a number of otherwise very puzzling observed features of the Homunculus nebula, if we borrow well-established shock physics and observational precedents from the class of SNe II_n. Finally, in §4 we discuss some implications for other eruptive transients, and we conclude with a summary in §5.

2 A SIMPLE WORKING MODEL: A DENSE WIND FOLLOWED BY AN EXPLOSION

2.1 Motivation

Two sets of different observations motivate the specific type of explosion-powered model suggested below, which is very different from the traditional picture of a super-Eddington wind usually discussed for η Car’s eruption (e.g., Davidson 1987; Davidson & Humphreys 1997; Owocki et al. 2004).

The first set of observations is that a number of different clues point toward an explosive component associated with the eruption of η Car. As noted above, several observations — like the high ratio of mechanical to radiated energy, the large mass and kinetic energy of the nebula apparently ejected in a very short time, the brief brightening events associated with periastron, and the extremely fast ($3000\text{--}5000 \text{ km s}^{-1}$) material seen in the ejecta around η Car — all point toward some sort of a brief explosion that was associated with the event. A super-Eddington continuum-driven wind could in principle supply the mass needed for the Homunculus over a ~ 15 yr time period (Owocki et al. 2004; van Marle, Owocki, & Shaviv 2008, 2009), but doing that and also producing high outflow speeds seems problematic. This is because one expects the effective escape speed from the star to drop as it approaches the Eddington limit

(Owocki & Gayley 1997; Owocki et al. 2004), and also because at such extreme mass-loss rates around $1 M_{\odot} \text{ yr}^{-1}$ or more that are required for a wind alone, the wind is in the regime of photon tiring¹, where much of the radiated energy is used to accelerate the mass (see Owocki et al. 2004; Owocki & Gayley 1997; van Marle et al. 2008, 2009). Thus, a relatively slow and heavy wind is generally expected, in contradiction to the very fast speeds with homologous expansion. Multi-dimensional effects may help simulations of super-Eddington winds reach the physical parameters of the 600 km s^{-1} Homunculus, but probably not the much faster material outside it. Adding an explosive component can explain the higher velocities that are observed, plus a number of other observations that we discuss in detail later on.

The second set of motivating observations is that many observers have noted that narrow H Balmer lines and other properties in spectra of core-collapse SNe IIn are very reminiscent of the spectrum of η Car. Objects like some of the most luminous and energetic SNe known (such as SN 2006gy), as well as stellar eruptive transients that are 4-5 orders of magnitude less luminous, all have aspects of their visual-wavelength spectra that appear similar to spectra of η Car. Many of these also exhibit evidence in the spectrum of some very fast material, even in LBV eruptions (like SN 2009ip; Smith et al. 2010b). Historically, this similarity may have caused genuine core-collapse SNe to be misclassified as η Car analogs, as in the case of SN 1961V (see Smith et al. 2011; Kochanek 2011), where early observers like Zwicky (1964) noted its similarity to η Car. This similarity in spectra includes recent reports of the spectrum of light echoes from the Great Eruption of η Car itself (Rest et al. 2012). With similar spectra produced over such a huge range of luminosity, it seems likely that CSM interaction may play an important role in more than just the most luminous SNe IIn (where CSM interaction is the only viable engine).

Moreover, the example of SNe IIn demonstrates that explosion kinetic energy which is converted to visual-wavelength radiation through CSM interaction can significantly boost the luminosity and extend the duration of the bright phases of the SN light curve. Indeed, the total radiated energy in the case of SN 2006gy was more than 10^{51} ergs in visual light alone, showing that the conversion of kinetic energy to visual light can be extremely efficient (Falk & Arnett 1977; Smith et al. 2010a; van Marle et al. 2010; Chevalier & Irwin 2011). This same mechanism should work efficiently for lower energy explosions as well.

2.2 CSM interaction powering the Great Eruption?

This section discusses a model for η Car's eruption that is akin to the standard model for SNe IIn, where an explosion produces a shock wave that expands into dense circumstellar material (CSM). A key ingredient is the presence of very dense CSM ahead of the shock wave, ejected by the star before the explosion. We consider two different potential origins for this pre-shock CSM in the sections to follow.

¹ The term ‘‘photon tiring’’ can be alternatively expressed as adiabatic cooling of the gas and radiation field.

Dense CSM slows the shock, and the resulting high densities in the post-shock region allow the shock to become radiative. With high densities and optical depths, thermal energy is radiated away primarily as visual-wavelength continuum emission. This loss of energy removes pressure support behind the forward shock, leading to a very thin, dense, and rapidly cooling shell at the contact discontinuity (usually referred to as the ‘‘cold dense shell’’, or CDS; see Chugai et al. 2004; Chugai & Danziger 1994). This CDS is pushed by ejecta entering the reverse shock, and it expands into the CSM at a speed V_{CDS} . In this scenario, the maximum emergent continuum luminosity from CSM interaction is given by

$$L_{CSM} = \frac{1}{2} \dot{M} \frac{V_{CDS}^3}{V_W} = \frac{1}{2} w V_{CDS}^3 \quad (1)$$

where V_{CDS} is the outward expansion speed of the CDS, V_W is the speed of the pre-shock wind, \dot{M} is the mass-loss rate of the wind, and $w = \dot{M}/V_W$ is the so-called wind density parameter (see Chugai et al. 2004; Chugai & Danziger 1994; Smith et al. 2010).²

Can this general scenario of CSM interaction for SNe IIn also be applied to η Car? The luminosity of the extended bright phase of the Great Eruption was of order $2.5 \times 10^7 L_{\odot}$. Most of the mass in this CSM interaction ends up in the CDS, and so V_{CDS} should correspond to the expansion speeds observed for most of the mass of the resulting Homunculus, which is about 600 km s^{-1} (Smith 2006). The observed luminosity of the Great Eruption would then require a wind density parameter of $w \simeq 10^{18} \text{ g cm}^{-1}$. This is similar to values of w required for luminous core-collapse SNe IIn. As long as η Car can supply pre-shock CSM of this density, then a CSM-interaction model is feasible to explain the Great Eruption luminosity.

In the CSM-interaction models explored below, we assume that the total mass involved in the CSM interaction is $20 M_{\odot}$, with $10 M_{\odot}$ in the first mass ejection (pre-eruption wind or explosion 1), and $10 M_{\odot}$ in the 1843/1844 explosion. While these values appear extreme, the choice is dictated by the observed mass of the Homunculus. Smith et al. (2003) measured a mass in the Homunculus of at least $12.5 M_{\odot}$, but noted that this was a likely lower limit due to the assumptions involved in deriving the total gas mass from observations of dust. Smith & Ferland (2007) derived a total mass for the Homunculus of $15\text{--}35 M_{\odot}$ from models to explain the density of the molecular hydrogen gas (mostly independent of the dust mass), and noted that values in the lower range of $15\text{--}20 M_{\odot}$ were favored. Gomez et al. (2010, 2006) derived a likely upper limit to the mass of around $40 M_{\odot}$ based on sub-mm observations of cool dust (this is a probable upper limit because some of this cool dust might be located outside the Homunculus). We therefore adopt a value of $20 M_{\odot}$ for the total mass in the Homunculus in these models.

² Note that this scenario where radiation escapes efficiently is somewhat different from a more extreme case where the radiation diffusion time is comparable to the expansion timescale, changing the shape of the light curve and requiring trapped photons to do significant work (Smith & McCray 2007; Chevalier & Irwin 2011; Falk & Arnett 1977).

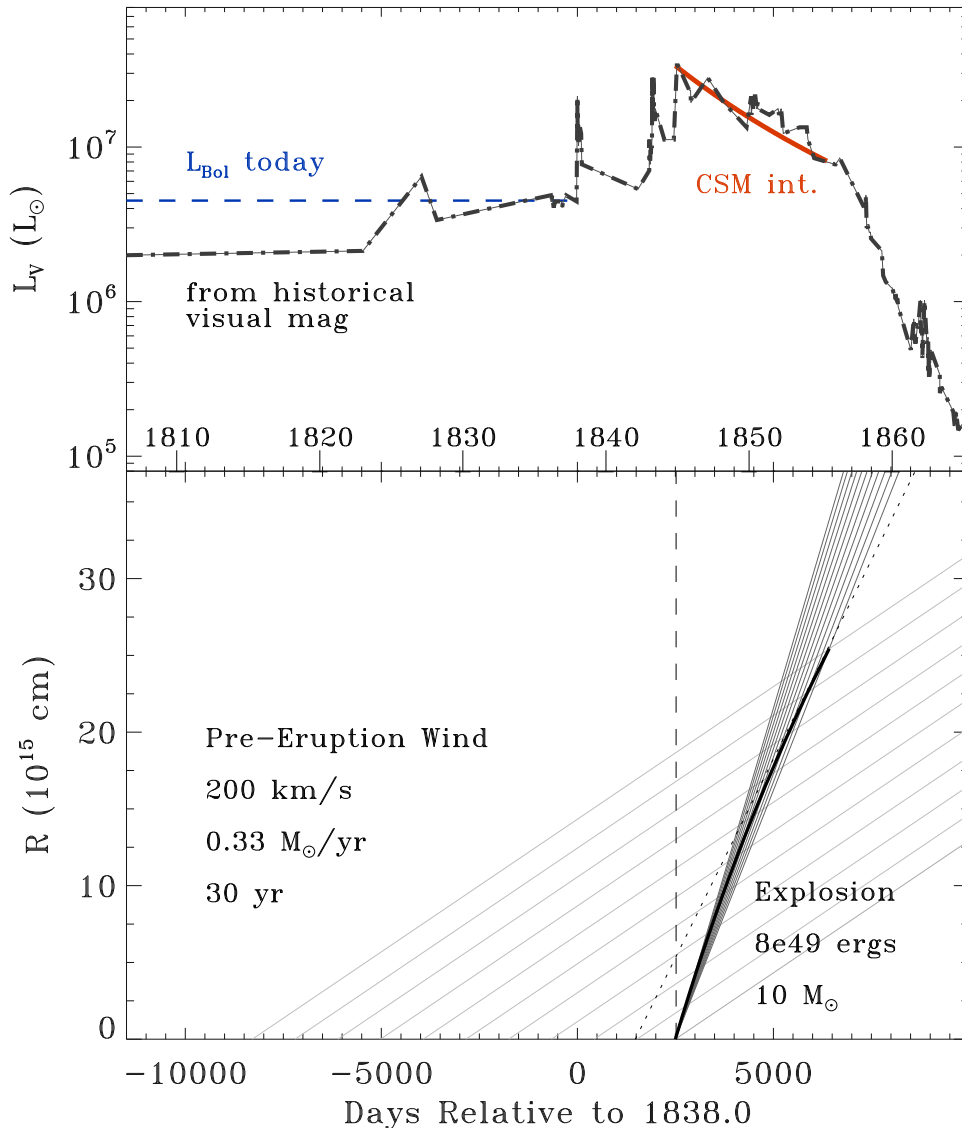


Figure 1. A CSM-interaction model for the Great Eruption of η Carinae. The top panel shows the historical visual-magnitude light curve of η Car (Smith & Frew 2011) converted from absolute visual magnitudes to solar luminosities. This uses no bolometric correction, which is probably close to being valid for around 1830-1860 (days -3000 to $+8000$ relative to 1838.0). Before 1830 the star was likely hotter than 7,000 K and so a bolometric correction is needed (the dashed blue line indicates its present-day bolometric luminosity), and after 1860 there is probably significant extinction from dust. The orange curve shows the luminosity generated by CSM-interaction in our favored model, with an 8×10^{49} erg explosion expanding into a dense wind. The bottom panel shows the radius as a function of time, indicating trajectories for the two main components of the model: (1) a steady continuum-driven wind with $\dot{M} = 0.33 M_{\odot} \text{ yr}^{-1}$ and $V_{\infty} = 200 \text{ km s}^{-1}$ ($10 M_{\odot}$ total) blowing for 30 yr prior to 1844.0, and (2) an 8×10^{49} erg explosion in 1844, ejecting $10 M_{\odot}$ at speeds ranging from 750 to 1000 km s^{-1} . The black solid curve is the resulting trajectory of the CDS, and the dotted black line marks the trajectory of the Homunculus that one would infer from today’s observed polar expansion speed. The trajectory of the CDS is calculated from conservation of momentum when the two components collide, and the resulting luminosity in the top panel is the difference in energy when momentum is conserved.

2.3 Pre-shock CSM produced by a wind

Let us first consider the simpler case where the required pre-shock CSM is supplied by a very dense but steady wind, occurring for at least a few decades before 1844. In some sense, this is not far from the traditional interpretation of LBV eruptions that invoke a super-Eddington wind phase to drive the mass loss. Here we assume that this wind supplied

much of the mass (about half), but very little of the kinetic energy of the eruption.

A strong pre-eruption wind phase has observational support, since the historical light curve shows that η Car was already in a long-duration eruptive state in the early 19th century (Smith & Frew 2011). The observed red-orange color of the star during the 1830s ($B - V = 0.7 - 1.2$ mag; Smith & Frew 2011), with a known line-of-sight reddening,

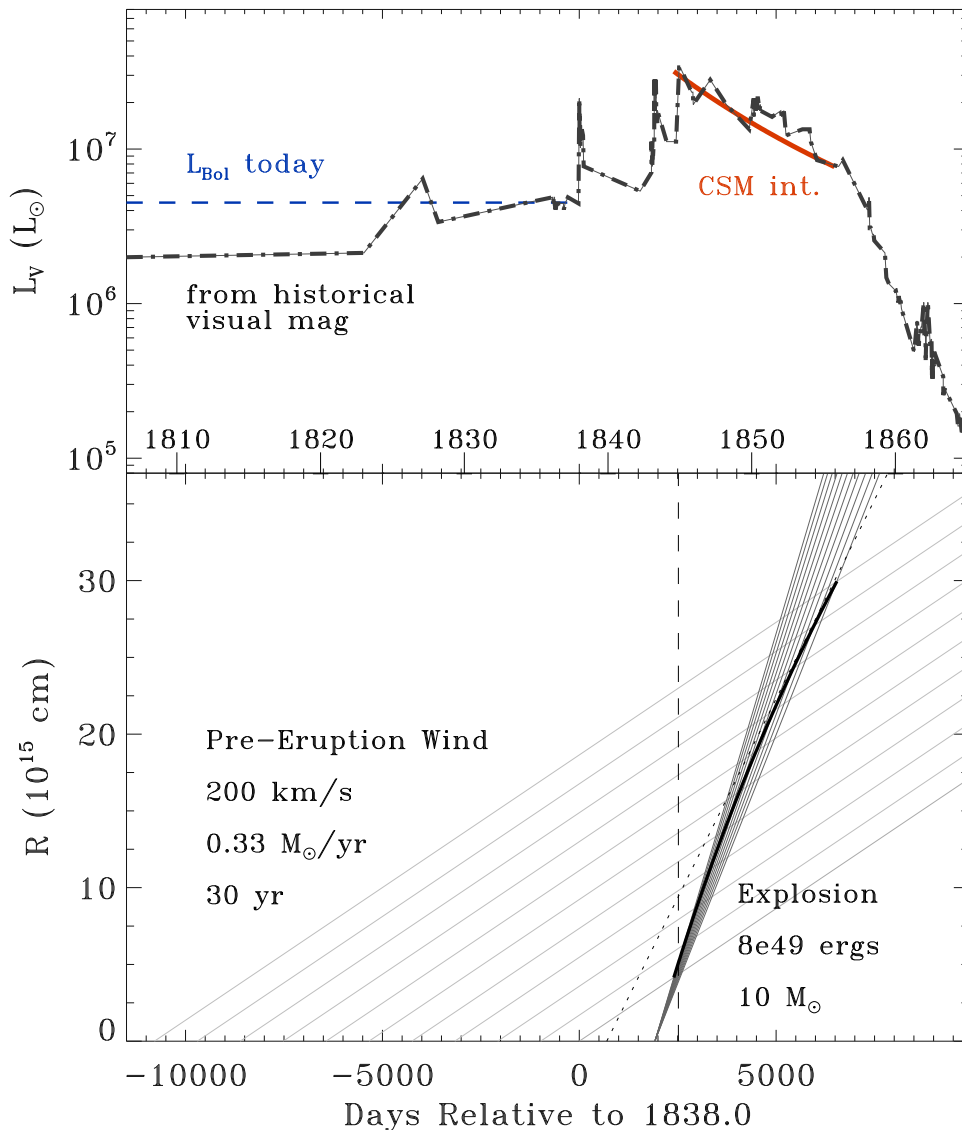


Figure 2. Same as Figure 1, but with slightly adjusted parameters in the times of ejection. Here the main explosion coincides with the 1843 periastron passage instead of at the time of the 1844 brightening, whereas we assume that the dense wind shuts off in 1838 at the previous periastron event. This is to provide a cavity so that the CSM interaction luminosity turns on after a delay, beginning in 1844. The resulting light curve is identical to Model 1. The purpose here is to illustrate that the model is not sensitive to the exact timing of the explosion (i.e. one can adjust the parameters slightly and still achieve a reasonable luminosity, providing that the CSM interaction begins at the onset of the brightening in 1844).

suggests that the star had a cool temperature of $\sim 7,000$ K (and hence, a small bolometric correction), and that its photospheric radius had swelled to be around 6–7 AU (Smith 2011). This is 7–10 times larger than the present-day radius, and would suggest a correspondingly smaller escape speed. With a present-day wind speed around 550 km s^{-1} (Hillier et al. 2001), the pre-eruption wind speed should then (naively) scale to about $160\text{--}220 \text{ km s}^{-1}$. Based on the observed properties in the 1830s, we therefore adopt a pre-eruption wind speed of order 200 km s^{-1} . This is not a unique requirement of the observations, but it is plausible.

It remains unclear if the emitting photospheric radius leading up to the eruption is the hydrostatic radius of the

star, or just a pseudo-photosphere in the wind for which a drop in V_{esc} is not necessarily expected. However, note that during the 1890 eruption, when direct spectra of η Car are available, the star exhibited a cooler F-supergiant-like spectrum and – more importantly – Doppler shifts of absorption lines seen in those spectra indicate an outflow speed of only 200 km s^{-1} (Whitney 1952; Walborn & Liller 1977). Humphreys et al. (1999) and others have commented that the properties of the star during the 1890 eruption were probably similar to those at the beginning of the Great Eruption, if one corrects for extinction from the Homunculus in 1890. Thus, there is a strong observed precedent for

Table 1. Adopted input parameters for Models 1 and 2: Pre-shock CSM produced by a wind.

Parameter	Units	Wind	Explosion
Mass	M_{\odot}	10	10
\dot{M}	M_{\odot}/yr	0.33	...
V_{exp}	km/s	200	750–1000
L_w	L_{\odot}	1.1×10^6	...
$E_{kinetic}$	ergs	4×10^{48}	7.7×10^{49}

the primary star having a slower and denser wind of 200 km s⁻¹ when it is in a cooler eruptive state.

For $V_W=200$ km s⁻¹, the corresponding mass-loss rate needed to produce the fiducial wind density parameter of $w \simeq 10^{18}$ g cm⁻¹ (see above) is roughly $0.3 M_{\odot} \text{ yr}^{-1}$. This mass-loss rate is extremely high, and is much higher than can be produced by normal line-driven winds (see Owocki et al. 2004; Smith & Owocki 2006; Aerts et al. 2004). It is, however, comfortably within the regime of continuum-driven winds that are mildly super-Eddington ($\Gamma = 2$ to 4; see Fig. 6 of Owocki et al. 2004), and that experience some degree of photon tiring. Such winds have been discussed extensively in connection to η Car and other LBVs (Shaviv 2000; Owocki et al. 2004; Owocki & Gayley 1997; van Marle et al. 2008, 2009), as well as compact objects (Joss et al. 1973; Quinn & Paczynski 1985; Paczynski 1990; Belyanin 1999). A mass-loss rate of a few $10^{-1} M_{\odot} \text{ yr}^{-1}$ is plausible, based on these studies of η Car. The photon-tiring limit (see Owocki & Gayley 1997), $\dot{M} = 2L/V_W$, is roughly $1.6 M_{\odot} \text{ yr}^{-1}$ for η Car’s present luminosity (and $V_W=200$ km s⁻¹), and would increase for higher values of L . This adopted pre-eruption wind used a luminosity $L_w = (1/2)\dot{M} (V_{\infty}^2 + V_{esc}^2)$ of roughly $2 \times 10^6 L_{\odot}$. If the apparent temperature for the pre-eruption star was around 7,000 K, as noted above, the bolometric correction was probably small, and so the *emergent* radiation in the 1830s was likely to be close to the star’s present luminosity of $\sim 4.5 \times 10^6 L_{\odot}$. This means that the actual luminosity was at least $7 \times 10^6 L_{\odot}$ and that at least 30% of the available radiation energy was used to accelerate the wind.

It is interesting to note that while slower wind speeds are one of the obstacles to explaining the creation of the Homunculus nebula with a wind acting alone, the slower speed is actually an advantage in the CSM interaction model because a slower pre-shock CSM increases the efficiency of converting shock kinetic energy into radiation. Adopting $V_W=200$ km s⁻¹ and $\dot{M} = 0.3 M_{\odot} \text{ yr}^{-1}$, we can then rewrite equation (1) as

$$L_{CSM} = 2.5 \times 10^7 \left(\frac{\dot{M}}{0.3} \right) \left(\frac{V_{CDS}}{600} \right)^3 \left(\frac{V_W}{200} \right)^{-1} L_{\odot}, \quad (2)$$

with \dot{M} expressed in $M_{\odot} \text{ yr}^{-1}$, and both V_{CDS} and V_W in km s⁻¹. Equation (2) shows that values of roughly $\dot{M} = 0.3 M_{\odot} \text{ yr}^{-1}$ and $V_W = 200$ km s⁻¹ are plausible for a scenario where an explosion being driven into a slow dense wind powers η Car’s Great Eruption luminosity. We consider this hypothesis below in more detail.

Equations (1) and (2) are somewhat idealized, since the value of V_{CDS} will become slower with time as the shock sweeps up more of the slow and dense CSM, and as the speed of explosion ejecta entering the reverse shock slows

as well (see, e.g., van Marle et al. 2010; Smith et al. 2010a; Chugai et al. 2004; Chugai & Danziger 1994). Thus, instead of the light curve showing a flat 10 yr plateau at $2.5 \times 10^7 L_{\odot}$, one might expect the luminosity to drop slowly with time (as is indeed observed).

This effect is explored using the model shown in Figure 1, where we calculate the relevant physical parameters at each time step. This model has two phases, as presumed above. Phase 1 is a dense continuum-driven wind that is active for 30 years preceding the explosion, with parameters of $\dot{M} = 0.33 M_{\odot} \text{ yr}^{-1}$ (chosen for convenience to yield a total mass of $10 M_{\odot}$ in the CSM) and a terminal speed of 200 km s⁻¹. One could adjust the wind speed, mass-loss rate, and duration of the wind slightly to produce a similarly dense and extended CSM, as long as it roughly obeys equation (2). Phase 2 is a dynamical explosion that occurs at the time of the main brightening in late 1844 (see Smith & Frew 2011), with a total kinetic energy of 7.7×10^{49} ergs, ejecting a total of $10 M_{\odot}$ in a Hubble-like flow with speeds ranging from 750 to 1000 km s⁻¹. The radial trajectories of the wind and explosion ejecta are shown in the bottom plot in Figure 1. The thick black curve shows the resulting trajectory of the CDS where parcels of mass from the two phases meet. Momentum is conserved at each time step in the collision, and the deceleration leads to a loss of kinetic energy. We assume that the difference between the initial and final kinetic energy in this collision is radiated away, and the radiated energy produces a corresponding emergent luminosity at each time step. The corresponding bolometric luminosity supplied by this collision is shown by the solid (orange) curve labeled “CSM int.” in the top panel of Figure 1. As shown in Figure 1, a simple CSM interaction model with the parameters listed in Table 1 provides an excellent match to the observed shape and magnitude of η Car’s light curve.³

The drop in luminosity at the end of this bright phase (around day 6000-7000 in Figure 1, or the late 1850’s) is not included explicitly in the calculated model. It can, however, be explained naturally with CSM interaction, as the shock/CDS overtakes the outer edge of the densest part of the slow continuum-driven wind (this is why we assumed a 30 yr duration for the wind). As the wind density parameter w drops, so does the CSM interaction luminosity. After exiting the dense slow wind, the expanding shock will presumably encounter a faster and lower density wind, corresponding to the star in its more normal state before the eruption began. Indeed, the fainter visual magnitudes before 1800 (Smith & Frew 2011) would suggest that the star was hotter, and therefore more compact with a higher escape speed (perhaps similar to the present-day wind). Faster CSM will lead to a lower CSM-interaction luminosity, as will a less dense wind. Alternatively, the luminosity may also drop because the speed of ejecta entering the reverse shock will slow down at late times and the shock loses power. Similar drops in luminosity are observed in SNe II_n that are thought to be powered by CSM interaction, such as SN 1994W (Chugai et

³ Note that we do not include a contribution from the pre-eruption stellar luminosity in the radiation energy budget of the eruption, because it is not clear that the star’s radiative output remains high when most of the star’s envelope is explosively ejected (i.e. the energy budget of the star must do work to rebuild the envelope after ejection).

al. 2004), SN 2009kn (Kankare et al. 2012), and SN 2011ht (Mauerhan et al. 2012; Roming et al. 2012). The formation of new dust grains may cause additional extinction, but this is not required to explain the initial drop in luminosity in the late 1850s, and observations are inadequate to constrain the influence of extinction. Dust formation in the context of CSM interaction is discussed below in §3.6.

The thin dotted line in Figure 1 shows the linear trajectory of the polar regions of the Homunculus that one would infer from present-day proper motions of the expanding nebula in images. From assuming ballistic motion of the nebula, one would infer an ejection date of 1842–1843 in this model, even though the explosion actually occurred in late 1844.

2.4 Pre-shock CSM made by a wind (variation)

In Figure 2 we show Model 2, which is almost identical to Model 1 except that we have adjusted the times of ejection somewhat to explore the observational consequences. This model has the explosion occurring at the periastron passage of 1843, instead of at the time of the main brightening in late 1844. This model may be attractive if the periastron passage instantly triggers the explosion, although we are not necessarily advocating this. In that case, to make the CSM interaction luminosity turn on in late 1844, as observed, one would need to turn off the wind to allow a relatively low-density cavity around the star. Model 2 (Figure 2) shows that if the dense wind is shut off at the time of the 1838 periastron passage, the delay in turning on the CSM-interaction luminosity matches the late 1844 brightening. The trajectory of the CDS in this model (dotted line in Figure 2) would lead a modern observer to infer an ejection date at the end of 1839, assuming linear motion.

The purpose here is not to advocate for this type of fine-tuning, but to demonstrate that varying the exact time of the explosion and wind properties by small amounts does not produce a major change in the light curve (i.e. one can make adjustments and produce the same result). This is because the key parameters are the slow pre-explosion wind speed, the high pre-explosion wind density, and the energy of the explosion. As we see below, significantly changing the nature of the mass ejection that produces the CSM does introduce significant changes to the light curve that are more difficult to reconcile with observations.

2.5 Pre-shock CSM made by a previous explosion

We also consider an alternative model (Model 3; Table 2) in Figure 3, where a sequence of two shells are ejected in 1838 and 1843 at periastron encounters when the secondary star plunges into the envelope of the bloated primary star (see Smith 2011; Smith & Frew 2011).⁴ The collision of two shells in this way is, in principle, similar to the model for SN 1994W suggested by Dessart et al. (2009), except that

⁴ Note that the two consecutive explosions of $10 M_{\odot}$ are adopted to calculate the resulting CSM interaction luminosity. As noted by Smith (2011), the energy of the secondary star plunging through the primary star's envelope is insufficient to power the mass ejection, so some additional (and unknown) energy input would be needed.

Table 2. Adopted input parameters for Model 3: Pre-shock CSM produced by a previous explosion.

Parameter	Units	Wind	Explosion
Mass	M_{\odot}	10	10
V_{exp}	km/s	420–480	650–1700
$E_{kinetic}$	ergs	2×10^{49}	1.5×10^{50}

SN 1994W was more luminous, shorter duration, and a more energetic event.

The interaction and emergent luminosity were calculated in the same way as above, but with the CSM provided by a previous explosion with a range of speeds rather than a steady wind with all matter ejected at the same speed. Adopted parameters are listed in Table 2. Figure 3 shows that a scenario with two sequential explosive shell ejections does not explain the observed light curve as well as an explosion crashing into a dense wind. It overproduces the luminosity at early times in the event, and far underproduces the luminosity at late times. This is because the higher velocities involved drain more kinetic energy at early times due to the V_{CDS}^3 dependence in Equation 1. In other words, at first the fastest ejecta from explosion 2 collide with the slowest ejecta from explosion 1, producing a high luminosity due to the large difference in speed — whereas at later times, the slowest ejecta from explosion 2 just barely overtake the fastest ejecta from explosion 1, so the deceleration and mass involved in each time step are much less severe, making it difficult to sustain a high luminosity in this model.

Moreover, this model requires significant and arbitrary fine-tuning in the velocity ranges of the two explosions, in order to match the observed duration of the bright event, unless some other radiative-transfer effects are important. The speeds that are needed to make the CSM interaction have the correct duration also result in smaller differences in speed, making the conversion of kinetic energy to radiation less efficient; this in turn places higher demands on the kinetic energy involved in the mass ejection (see Table 2), as compared to the wind + explosion model. To make this double-explosion scenario produce the correct radiated luminosity, one would need to carefully redistribute the mass in each velocity range, and in a different way for both explosions (i.e. relatively more mass ejected at high velocity in the 1838 explosion, and relatively more mass at lower speeds in the 1843 explosion). The trajectory of the CDS in this model (dotted line in Figure 3) would lead a modern observer to infer an ejection date in 1839, assuming linear motion.

This double-explosion scenario therefore seems more difficult to accommodate than the wind + explosion model presented in Figure 1, even though the sequential ejection of two shells at two periastron events may provide a somewhat compelling physical motivation. The implication is that instead of dominating the mass ejection and energetics, periastron passages may play an important role in modifying the geometry (see §3.5).

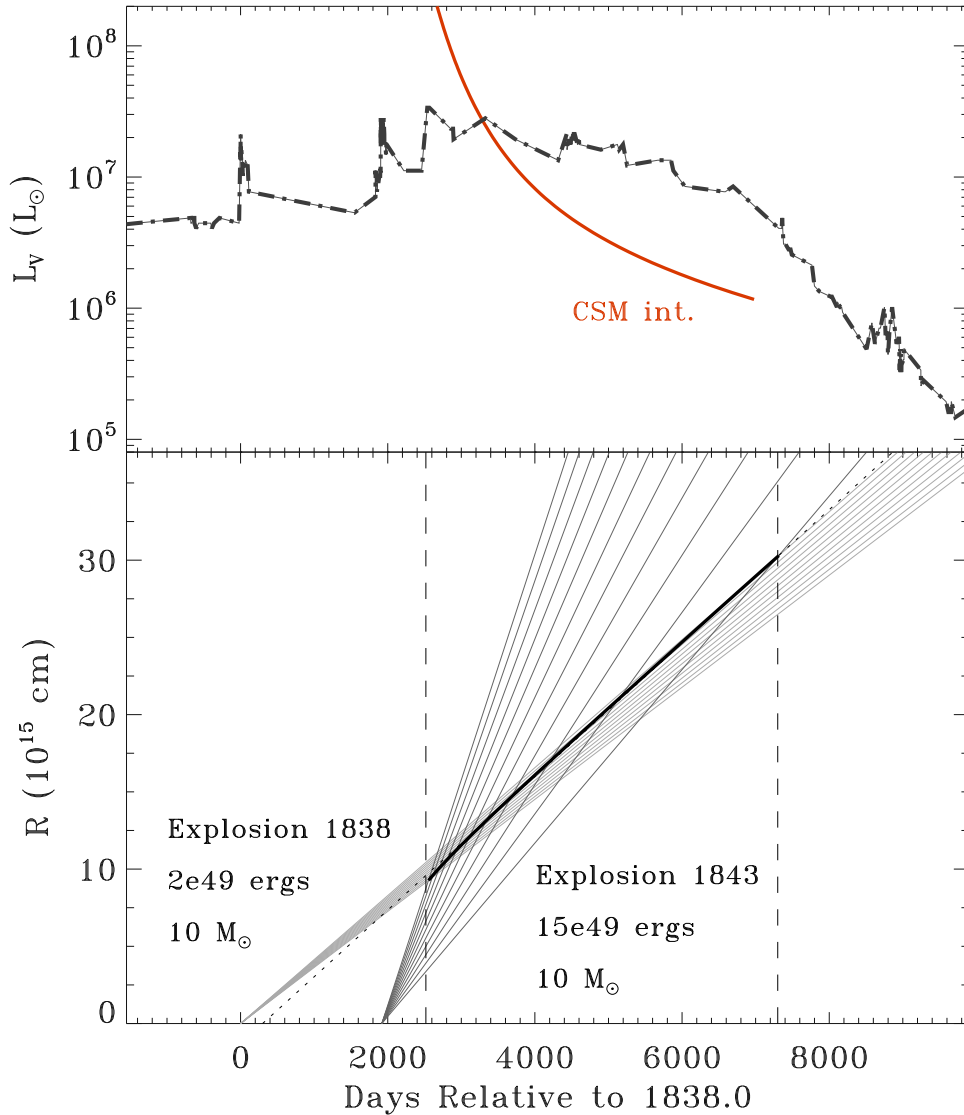


Figure 3. Same as Figure 1, but for an alternative model with two sequential explosive shell ejections that collide, instead of an explosion expanding into a dense wind. This model produces a less satisfactory match to the emergent luminosity observed in the eruption.

2.6 Levels of complexity

The favored model above (Model 1; Figure 1) is quite simple. One can, of course, fiddle with various parameters to adjust the resulting light curve. For example, the pre-eruption wind speed V_W may not be constant with time, or its mass-loss rate and wind density may increase or decrease as the star brightens in the years leading up to 1844 (see Smith & Frew 2011). Similarly, the mass in the explosion may not have been distributed evenly across the range of expansion speeds. The goal here was to demonstrate that even the simplest assumptions can provide a reasonable account of the high luminosity and long duration of the Great Eruption. This simple test should be followed by more rigorous numerical hydrodynamical simulations that more accurately account for radiative transport with high optical depths, which may be important at early times.

In principle one could get a similar result by having a

dense slow wind that is followed by an ever increasing wind speed. Such a scenario would still produce a thin expanding shell that looked as though it had a single age. This may apply to some extragalactic LBV-like transients, since these are seen in large variety (see Smith et al. 2011). For example, the object UGC 2773-OT also has been having an LBV-like eruption that is taking place over more than 10 years, although it has a much smoother light curve and no signs of a fast blast wave in spectra (Smith et al. 2010b). Ultimately, though, this fast wind that follows the slow wind must carry a large amount of kinetic energy in order to explain the visual light curve through CSM interaction. Most of the other extragalactic LBV-like transients have shorter duration (less than 1 yr) and so steady winds are unlikely to be suitable power sources.

Geometry adds another level of complexity, since one may account for variations in mass and speed with latitude, as observations of the Homunculus require (Smith 2006).

Soker (2007; and references therein) has advocated a model wherein eruptive mass loss from the primary caused a dense wind that is accreted onto the secondary star in a binary system, in order to explain the Great Eruption of η Car and the formation of the Homunculus nebula. In that model, the radiative luminosity of the eruption is assumed to result from accretion luminosity as $8 M_{\odot}$ is accreted from the primary wind onto the companion star through Bondi-Hoyle accretion over a few years, and the bipolar shape of the Homunculus is caused by a fast collimated wind or jet assumed to be launched by the secondary as a result of that accretion. A physical difficulty of this model is that in order to explain the radiative luminosity of $2.5 \times 10^7 L_{\odot}$ during the eruption, the $\sim 30 M_{\odot}$ companion star must accrete material at $\gtrsim 20$ times the Eddington accretion rate, and accreting such a large amount of matter in such a short time requires extreme parameters for the primary eruption that seem to overwhelm any other energy source. Some accretion onto the companion may occur, and the impact on the geometry may be relevant, but it seems impossible that accretion is the power source for the emitted luminosity. Instead, one can envision a version of the CSM interaction model discussed above, where instead of an explosion, we have a strong and fast wind acting over a short time, which overtakes a slow dense wind emitted previously. Making this into a collimated fast wind or a jet is just a matter of the latitudinal structure of the fast wind, and the arguments above would still hold. The different implications for the underlying physical cause of the eruption are important, of course, but the end result of the CSM interaction may be very similar. Thus, it seems plausible that even in a model that invokes a collimated fast wind or jet to help explain the geometry, it is still quite likely that CSM interaction is the engine that powers the radiated luminosity of the Great Eruption.

3 OBSERVED CONSEQUENCES

The Homunculus nebula around η Car is one of the most intensively observed objects in the sky (see the recent review by Smith 2009). Its linear expansion extrapolates back to an ejection date during the Great Eruption in the 1840s (Morse et al. 2001; Smith & Gehrz 1998; Currie et al. 1996), and as such, it provides some of our most crucial information about the physics of the eruption. The amount of detailed information provided by the Homunculus is almost too rich: While it is sometimes lamented that invoking binary systems allows theorists to “ascend into free parameter heaven” (Gallagher 1989), η Car is a case where so much detailed information is available that theorists may be weary of descending into an observationally overconstrained purgatory that halts progress. There are many peculiar mysteries associated with the Homunculus, each presenting its own challenge to one theory or another.

The approach below is to suggest that what works for traditional SNe IIn also seems to work well for η Car and the Homunculus. Essentially, we are suggesting that the Great Eruption of η Car behaved like a scaled-down (in kinetic and radiated energy) version of the CSM interaction in a Type IIn supernova, and that the observed properties of the Homunculus can be understood as the end result of that CSM interaction. The energy input comes from a weaker

non-terminal explosion of unspecified origin instead of Fe core-collapse, but otherwise the shock physics is similar to a SN IIn. A number of well-established theoretical and physical precedents for SNe IIn can explain outstanding observational mysteries associated with the Homunculus, as outlined below.

3.1 Ratio of the kinetic energy of the Homunculus to the total radiated energy of the Great Eruption

The first strong clue that the Great Eruption behaved more like an explosion than a normal wind was its high observed ratio of kinetic energy to radiated energy ($\zeta = E_k/E_{Rad}$), which is substantially larger than unity (Smith et al. 2003). It may be possible to achieve $\zeta > 1$ with a continuum-driven wind that suffers considerable photon tiring (Owocki et al. 2004; van Marle et al. 2008, 2009), by using more than 2/3 of the available radiation energy budget to accelerate the wind (i.e. including potential energy, the luminosity required to accelerate the wind is $L = M(V_{\infty}^2 + V_{esc}^2)/2$), with the emergent radiation then being considerably less than the total. However, a ratio of $\zeta \gtrsim 1$ is also a natural consequence of strong CSM interaction, as seen in SNe IIn (Falk & Arnett 1977; Smith & McCray 2007; Chevalier & Irwin 2011). In a CSM-interaction model, the efficiency of converting kinetic energy into radiation depends on the change in velocity as the freely expanding ejecta (V_{ej}) cross the reverse shock and decelerate to the speed of the CDS (V_{CDS}), as well as the relative amounts of mass in the pre-shock CSM (M_{CSM}) and in the explosion ejecta (M_{ej}). For $M_{CSM} \geq M_{ej}$ and $V_{CDS} \ll V_{ej}$, the efficiency can approach 100%, for $M_{CSM} \approx M_{ej}$ and $V_{CDS} < V_{ej}$, the efficiency can range from a few per cent to roughly 50%. If $V_{CDS} \simeq V_{ej}$ then the efficiency is very low, and of course, if $V_{CDS} \geq V_{ej}$ there is no CSM interaction. So, as long as the pre-1843 wind was dense and slower than the explosion ejecta, CSM interaction is inevitable and an efficiency of converting kinetic energy into radiation of $\sim 25\%$ is easily achieved. Numerical simulations for SN IIn CSM interaction have verified this (van Marle et al. 2010).

3.2 Double-shell structure of the Homunculus

A clearly delineated double-shell structure exists in the Homunculus, seen in tracers of dust (Smith et al. 2003) as well as in different emission lines that trace different densities and ionization levels (Smith 2006, 2002; Smith & Ferland 2007). Most of the mass (at least 12-15 M_{\odot}) resides in a geometrically thin outer shell ($\Delta R < 0.05R$), whereas about 10% of the mass resides in a geometrically thicker ($\Delta R \simeq 0.2R$) but optically thinner inner shell. The thin outer shell has cooler dust at ~ 140 K, whereas the inner shell has warmer grains that are closer to 200 K. Also, the outer shell has neutral and molecular gas (depicted as red-orange in Figure 4), whereas the inner shell has neutral atomic H and singly ionized metals like Fe^+ (depicted as blue in Figure 4). The thin outer shell and thicker inner shell are also traced by UV absorption lines, with different velocity widths and ionization levels in the two zones (Nielsen et al. 2005; Gull et al. 2005). Smith & Ferland (2007) showed that the observed ionization

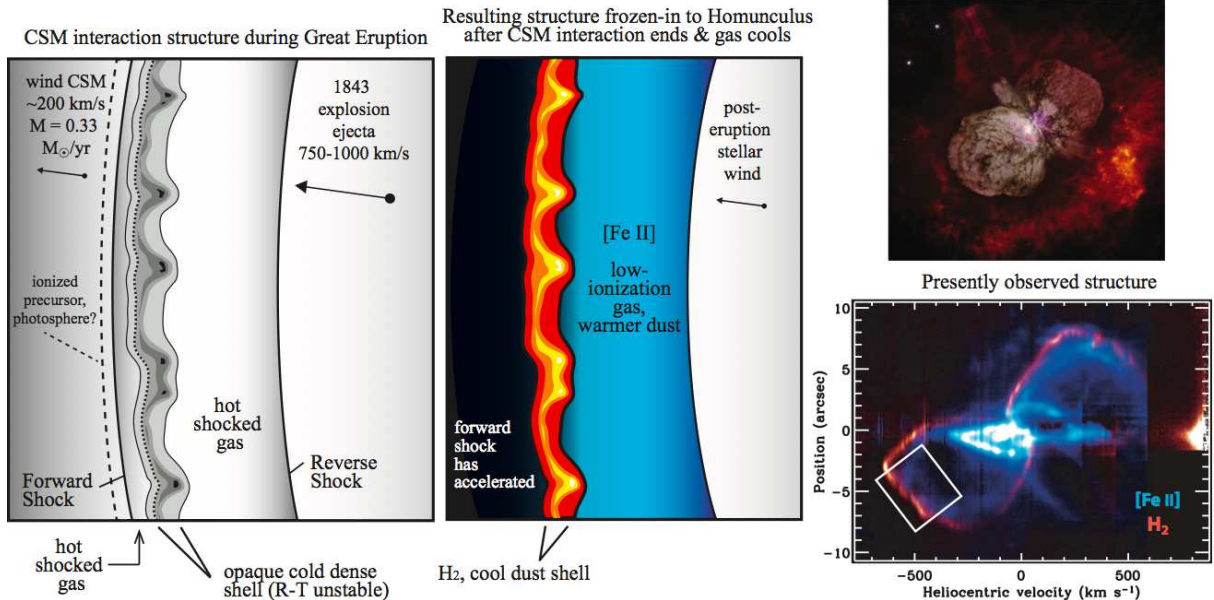


Figure 4. Illustration of how CSM interaction determines the presently observed structure in the Homunculus. The left panel shows a typical forward-shock/reverse-shock structure that arises in CSM interaction, as is often depicted for SNe IIn (this is adapted from a sketch for SN 2006tf in Smith et al. 2008a). A cold dense shell forms at the contact discontinuity between shocked CSM and shocked ejecta, which is Rayleigh-Taylor (RT) unstable (Chvalier & Fransson 1994). The middle panel shows the resulting density and ionization structure after the CSM interaction period ends. The CDS contains most of the mass in a geometrically thin shell; it has cooled to form dust and molecules, and is optically thick to UV radiation so that dust remains relatively cool. The geometrically thicker inner shell corresponds to some of the reverse-shocked ejecta that has cooled to have neutral H but ionized metals, and the dust is warmer as it is exposed to the full luminosity of the central star. The forward shock accelerated to higher speeds and reached much larger radii when it passed the outer boundary of the dense CSM shell. The volume interior to the [Fe II] shell is filled with post-eruption stellar wind. The two panels on the right depict the presently observed structure of the Homunculus; on the top is an *HST* image showing the “mottled” structure of the polar lobes (see Morse et al. 1998; Smith et al. 2004), which we associate with RT instabilities in the CDS, and the lower panel shows a position-velocity plot of 2.122 μm H₂ and 1.644 μm [Fe II] emission observed with the Phoenix spectrograph on Gemini South (Smith 2006). The white dashed box in the lower right highlights the double-shell structure that is sketched in the middle panel.

structure and dust-temperature stratification in the walls of the Homunculus can be explained naturally by radiative excitation (not shock excitation, as is usually assumed for gas emitting near-IR H₂ and [Fe II] emission), as long as the outer shell has an abrupt increase in density compared to the inner shell. The origin of that density stratification, however, was not explained.

We propose that even though the currently observed H₂ and [Fe II] emission is not *powered* by shock excitation, the density stratification that gives rise to this emission *is* the result of shocks. To clarify, we suggest that all the relevant CSM interaction and shock heating occurred in the 10-15 years after 1843. The relevant CSM-interaction shock structure during that event is depicted in the left panel of Figure 4, which is the same as for a generic SN IIn (from Smith et al. 2008a; see also Chugai & Danziger 1994; Chugai et al. 2004; Chevalier & Irwin 2011; Chevalier & Fransson 1994). After that time, the CSM interaction basically stopped⁵ because the post eruption wind ($V_W \simeq 550 \text{ km s}^{-1}$) had a speed comparable to or slower than the CDS and its mass-loss rate was insignificant. Therefore, the double-shell density structure corresponding to (1) the CDS, and (2) to the thicker shell between the CDS and the reverse shock were es-

entially “frozen-in” to the expanding structure. The structure is frozen in because the gas cools rapidly to 7,000 K and lower (dust and molecules form), so the sound speed is much lower than the bulk expansion speed of 600 km s^{-1} and the flow is ballistic. The “frozen in” density structure in coasting ejecta is a common feature of simulations of spherical stellar explosions in a density gradient (e.g., Fryxell, Mueller, & Arnett 1991). The H₂ and [Fe II] emission structure we see today comes from coasting radiatively-excited gas at different densities and with different ionization/dissociation properties; shock excitation no longer plays a relevant role in the energy balance.

3.3 The apparent Hubble-like flow

The main structural result of CSM-interaction with a radiative shock is the formation of a dense and thin CDS, as noted above. The trajectory of the CDS in our model is shown with the thick black curve in Figure 1, and its expansion is nearly linear during the eruption, with a final speed of about 530 km s^{-1} in this model. When the most active phase of CSM interaction ends, we have about $20 M_\odot$ located in this fast-moving CDS. Since CSM interaction ends, this massive CDS will simply coast unless it sweeps up a mass that is comparable, or until it encounters a high-pressure region. The CDS cooled quickly and will expand very supersonically and bal-

⁵ Although see §3.7.

listically for the 150 years after that, to be observed as the Homunculus with the Hubble-like expansion we see today (Morse et al. 2001; Smith & Gehrz 1998; Currie et al. 1996). The pre-eruption wind and post-eruption wind have similar speeds and orders of magnitude lower density, so they do not cause any perceptible acceleration or deceleration of the shell after 1860. Thus, even though the true mass loss was spread over a period of almost half a century, the fact that it was swept-up into a thin shell through CSM interaction (over a short time period that ended long before any observations used to measure proper motions) makes it appear as if all the mass in the Homunculus was ejected instantaneously. In this model, the ejection date one would measure is in 1842-1843, as noted previously. Thus, renewed investigations of the proper motion of the Homunculus can provide an important test of when the explosion actually occurred.

3.4 Mottled structure of the polar lobes in high-resolution images

A very complex web of dark lanes and bright cells is seen on the face of the south-east polar lobe of the Homunculus nebula, shown in the upper right image in Figure 4. The fine details of this structure were first seen in refurbished *HST* images of η Car (Morse et al. 1998; although see also Duschl et al. 1995; Currie et al. 1996; Smith et al. 2004). Many admirers of η Car have since been perplexed by this complex network of structure, resorting in some cases to vegetable comparisons or analogies to Solar granulation in lieu of a physical mechanism. This structure has no obvious explanation in a wind-only origin for the Great Eruption. While one does expect complex inhomogeneities in a super-Eddington wind (Shaviv 2000; Owocki et al. 2004), one does not expect these structures to persist at the same locations and size over 10 years during the eruption. Moreover, a wind-only mechanism would not give rise to the sudden changes in outflow that are required for the instabilities at a sharp interface like this. On the other hand, structures akin to this are a natural outcome of Rayleigh-Taylor (R-T) instabilities that occur in a thin shell at the contact discontinuity between a forward and reverse shock in CSM interaction (e.g., Chevalier & Fransson 1994). Such structures — including the nonlinear thin-shell instability (Vishniac 1994) and the impulsive case of R-T known as Richtmyer-Meshkov instabilities (Richtmyer 1960; Meshkov 1969) — are seen in a wide array of hydrodynamic simulations of shock-ISM collisions and wind-wind interaction (i.e. planetary nebulae; e.g., Frank & Mellema 1994; Mellema & Frank 1995; Fryxell et al. 1991), including some of those performed for η Car (e.g., Langer et al. 1999).

We propose that R-T instabilities (or Vishniac and Richtmyer-Meshkov instabilities) gave rise to a complex network of cells and filaments in the CDS with typical azimuthal size scales of a few per cent of the radius (roughly comparable to the thickness of the CDS). A key difference in this scenario compared to previous interacting-winds simulations of the Homunculus (Frank et al. 1995, 1998; Dwarkadas & Balick 1998; Langer et al. 1999) is that the shock is highly radiative (as it must be to produce the emergent luminosity of the Great Eruption), and the cooling causes material behind the forward shock to collapse into an extremely thin cold dense shell (CDS). This is the standard interpretation

for SNe IIn. As a result, the instabilities in the CDS have a much smaller radial extent than in most interacting winds scenarios, more appropriate for the very thin molecular layer of the Homunculus (Smith 2006). An extremely thin CDS corrugated by instabilities is seen in simulations of SN IIn collisions with significant cooling (van Marle et al. 2010). In η Car, this complex structure was determined only during the 10-15 years of active CSM interaction during the Great Eruption; when the CSM interaction stopped and the ejecta rapidly cooled, this structure was again “frozen-in” to the ballistically expanding shell for the next 150 years. The post-eruption wind could have little influence on even the small-scale structure of the polar lobes, since the wind density dropped by more than three orders of magnitude and had a similar expansion speed. Along with rapid cooling came dust formation in these R-T cells and filaments in the CDS, discussed below. That distribution of dust gives rise to the structure seen on the surfaces of the polar lobes in *HST* images, since the visual-wavelength light from the Homunculus is dominated by photons scattered off dust grains.

Some observers have noted that the complex structure on the side walls of the north-west polar lobe that we can see is different from that on the face of the south-east polar lobe (e.g., Morse et al. 1998). This difference may also be line with expectations of CSM interaction, since the side walls of the polar lobes have oblique shocks that may be dominated more by Kelvin-Helmholtz (K-H) instabilities rather than face-on R-T instabilities. The transition between the two regimes appears to occur at latitudes of roughly 45° .

3.5 Bipolar shape of the Homunculus

In principle, the bipolar shape of the Homunculus has already been explained theoretically in numerical simulations (Frank et al. 1995, 1998; Dwarkadas & Balick 1998; Langer et al. 1999; Gonzalez et al. 2004, 2010). These simulations involved a scenario of a fast wind blowing into a slow dense wind with an equatorial density enhancement (or a bipolar fast wind blowing into a spherical slow wind in the case of Frank et al. 1998). While these simulations adequately reproduce the overall bipolar *shape* of the Homunculus, there are some problems reconciling them with detailed observations (see Smith 2006). In general, the post-eruption wind of $1000\text{-}2000\text{ km s}^{-1}$ (which is faster than the observed post-eruption wind) overtakes a slower pre-eruption wind, shaping the nebula over a period of $\sim 100\text{-}150$ years. The adopted mass-loss rates result in a Homunculus mass that is an order of magnitude too small. This has led to alternative suggestions of an intrinsically bipolar wind during the Great Eruption with a much higher mass-loss rate, where the bipolar shape and latitudinal mass distribution result from the latitudinal variation of escape speed and mass-loss rate on a rotating star (Dwarkadas & Owocki 2002; Owocki et al. 1996, 1998; Owocki & Gayley 1997; Owocki 2003), which in principle also matches the observed shape (Smith 2002, 2006).

The scenario advocated here has some overlap with aspects of interacting-winds simulations (especially with Frank et al. 1995), except that instead of a post-eruption wind to inflate the Homunculus acting over a century, we adopt an explosion that impulsively accelerates the dense CSM/wind, and the mass and kinetic energy involved are much higher.

This causes a key difference between our proposed scenario and these interacting winds models, which is that *the shaping of the nebula occurs over only 10-15 yr*. The collision conserves momentum, and the loss of energy to radiation over this short time period gives rise to the extra luminosity of the Great Eruption, which is not included in any of the previous interacting-winds models. After about 1860, the central star presumably returns to its normal (weaker, present-day) wind and has little influence, in contrast to the interacting winds models.

What about the equatorial density enhancement required in these models? Observations of the Homunculus show that most of the mass is located over the poles, not in the equator (Smith 2006), and proper motions show that the extended equatorial skirt is not an older feature that was pre-existing around the Homunculus. This is problematic for models that create the bipolar shape with a fast wind continuously sweeping into an older and extended disk-like wind. In simulations by Dwarkadas & Balick (1998), however, a very small (10^{14} cm) torus surrounded the star before the eruption; this was sufficient to collimate and deflect mass into a bipolar flow, and the torus was destroyed in the interaction. Acting on such small size scales (where photon trapping will be important), this is similar to having an intrinsically bipolar explosion, at least as far as larger size scales and coasting trajectories are concerned. Perhaps a very compact slow torus could have been created during repeated periastron passages in 1838 and 1843, because during these periastron events the secondary star must have plunged into the bloated photosphere of the primary (Smith 2011). Brief 100-d peaks in luminosity were observed at times of periastron before the Great Eruption (Smith & Frew 2011). Simulations of this stellar collision would be very interesting, in order to determine the expected geometry. From studies of the central binary system, it has been established that the orbital plane of the binary is in fact the same as the equatorial plane of the Homunculus (Madura et al. 2012). The explosion geometry resulting from the internal distribution of angular momentum in the star’s envelope (see Balbus & Schaun 2012) and the time-dependent tidal influence of the nearby companion star are essentially unexplored in this context.

The extended “equatorial skirt” is prominent in *HST* images of the Homunculus (see Figure 4), and this structure is almost unique to η Car — generally equatorial features like this are not seen in planetary nebulae. Some ideas have been proposed to explain the creation of a flat equatorial skirt concurrently with the lobes in a super-Eddington eruption (Smith & Townsend 2007; Shacham & Shaviv 2012). However, we also point out that the equatorial skirt seen in *HST* images is somewhat illusory. Mid-IR images of thermal emission and some emission-line spectroscopy reveal that the equatorial skirt actually contains very little mass (Smith et al. 1998, 2002, 2003; Polomski et al. 1999; Smith 2002, 2003, 2008; Zethson et al. 1999; Hartman et al. 2004), and may result more from preferential illumination than from an equatorial density enhancement. Light escaping through a clumpy equatorial torus at the pinched waist of the Homunculus may explain the radial streaks with escaping beams of starlight. Thus, the existence of the equatorial skirt does not place important constraints on the geometry of CSM interaction.

3.6 Rapid and efficient dust formation

Massive dust shells are a commonly observed property of LBVs, and the dusty Homunculus of η Car is the best studied. Kochanek (2011) has discussed the efficient formation of large dust grains in an eruptive LBV wind, requiring very high mass-loss rates above $10^{-2.5} M_{\odot} \text{ yr}^{-1}$. In general, the formation of dust in a constant-velocity wind places strong demands on the density and mass-loss rate, which for hot stars can only be accomplished in the super-Eddington winds envisioned for LBV eruptions.

However, there is another way to trigger efficient and rapid dust formation that involves explosive mass loss rather than winds, and it has a well-established observational precedent. Namely, SNe with strong CSM interaction are observed to rapidly form copious amounts of dust in their post-shock layers. The first well-established case was SN 2006jc, which simultaneously (beginning only 50 days after explosion) showed IR excess from newly formed hot dust, increased fading in its visible light curve, and the characteristic blueshift of its narrow emission lines formed in CSM interaction (Smith et al. 2008b). SN 2006jc was a peculiar Type Ibn explosion (weak H lines), but a number of SNe IIn have shown the same post-shock dust formation (Smith et al. 2009, 2008a, 2012; Pozzo et al. 2004; Fox et al. 2009, 2011; Mauerhan & Smith 2012). The *formation* of dust in shocks is perhaps somewhat surprising, since one normally expects fast SN shock waves to destroy dust. The key difference in SNe IIn is that the CSM is very dense and the shock is slower and radiative. The efficient radiation from the shock also provides efficient cooling. In turn, the cooling removes pressure support and the forward shock collapses to a CDS, with densities above 10^{10} cm^{-3} . The higher densities from shock compression and lower temperatures from enhanced cooling of the radiative shock then lead to efficient dust formation.

Particle densities of order 10^{10} cm^{-3} are required for nucleation of dust grains (e.g., Clayton 1979), a condition which is met in the cold dense shells of SNe IIn that are observed to form dust. In the free expansion that has dominated the Homunculus in the 150 years since the end of the Great Eruption, the density in the Homunculus should drop as the radius increases, scaling roughly as $\rho \propto r^{-3}$. Since the ejecta are in linear expansion during this time, we can also expect $\rho \propto t^{-3}$. At the present epoch, densities of $\sim 10^7 \text{ cm}^{-3}$ are required in the thin outer shell of the Homunculus in order for H_2 to survive (Smith & Ferland 2007). Scaling from the present epoch ~ 160 years after the initial explosion in 1843 to just 10 years after (when CSM interaction ended), the density in the thin outer shell must have been 16^3 times larger, or a few $\times 10^{10} \text{ cm}^{-3}$. These densities are sufficient for dust nucleation. The gas temperature must also drop below ~ 1500 K, but this is easily achieved as the luminosity drops in the late 1850s and early 1860s.

The resulting physical parameters in the cooled, dense post-shock gas in CSM interaction satisfy the same conditions of temperature and density as very dense LBV winds that are thought to rapidly form large dust grains. The CSM-interaction mode of post-shock dust formation has a clear advantage over the constant-velocity wind hypothesis (Kochanek 2011), however, which is that in CSM interaction, the dust is expected to reside in a very thin shell cor-

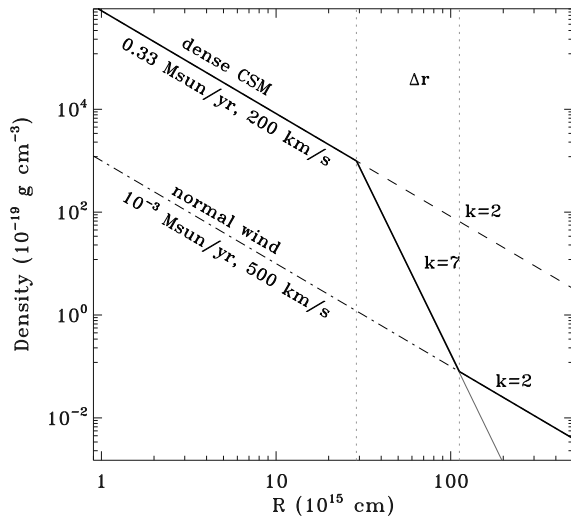


Figure 5. Density as a function of radius. The dashed line and dot-dashed line represent densities for two different mass-loss rates with $\rho \propto r^{-k}$ and $k=2$ (i.e. steady winds). One represents the strong continuum-driven wind leading up to the eruption in Models 1 and 2, with $\dot{M}=0.33 M_{\odot} \text{ yr}^{-1}$ and $V_W=200 \text{ km s}^{-1}$, and the other is for the wind of η Car in its normal (pre- and post-eruption) state, with $\dot{M}=10^{-3} M_{\odot} \text{ yr}^{-1}$ and $V_W=500 \text{ km s}^{-1}$. The thick black line shows a possible example of the transition between the two (see text), which has a much steeper density gradient with $k=7$ if we assume that the smooth transition took an additional 30 yr. This is the pre-shock density at about 10-15 yr after the explosion, appropriate for the time when the forward shock reaches the outer extent of the dense CSM. The pre-shock density drops by a factor of $\sim 10^4$ over a range of Δr in radius (Δr depends on how quickly the dense wind turned on leading up to the eruption, but is unknown).

responding to the CDS, as observed for η Car (Smith et al. 2003) and many other LBVs. This may be a significant obstacle for the idea of dust formation in a long-duration (~ 100 yr) wind proposed recently by Kochanek (2012) to explain the 20th century light curve of η Car.

Efficient dust formation in shocks has other precedents besides SNe II as well. In particular, the colliding winds of Wolf-Rayet binaries with WC stars form dust very efficiently due to the compression of the shock (see Crowther 2007). In fact, η Car itself provides an observed example of this phenomenon in its present-day state, since it shows episodes of enhanced dust formation in the colliding wind shock of the binary system during periastron passages (Smith 2010).

3.7 Some very fast material in a blast wave outside the Homunculus

The perplexing structure in η Car's ejecta continues outside the Homunculus. The so-called “outer ejecta” are a complex network of ionized, N-enriched condensations that appear to have been ejected centuries or millenia before the 19th century Great Eruption (Walborn 1976; Walborn et al. 1978; Walborn & Blanco 1988; Davidson et al. 1982, 1986; Meaburn et al. 1996; Weis 2001; Smith & Morse 2004; Weis et al. 1999, 2004; Smith et al. 2005). The dense condensa-

tions seen in images are expanding away from the star with typical speeds of a few 10^2 km s^{-1} .

There is, however, also evidence for much faster material that was ejected more recently, in the form of the long “whiskers” or “strings” seen in *HST* images (Morse et al. 1998; Weis et al. 1999, 2004), which are expanding radially with speeds of $\sim 1000 \text{ km s}^{-1}$, as well as the fastest material moving at $3000\text{-}5000 \text{ km s}^{-1}$ (Smith 2008) that is seen only in long slit spectra because it is Doppler shifted out of the narrow *HST* imaging filters. This fast material resides outside the Homunculus but inside the dense “outer ejecta” condensations mentioned above. Smith (2008) suggested that this fast material must arise from a blast wave from the Great Eruption, and that the collision between this very fast material and the slower and older condensations in the outer ejecta gives rise to the soft X-ray shell seen around η Car (Seward et al. 2001; Corcoran et al. 1995, 2004).

In the CSM-interaction interpretation advocated here, this outer soft X-ray shell would represent the current location of the forward shock. The reason that the radius of the forward shock is so much larger than the radius of the Homunculus now is that the forward shock accelerated when it encountered a steep density gradient at the outer boundary of the dense CSM, leaving the ballistically expanding CDS (and hence the Homunculus) behind. This situation is analogous to a rarefaction wave that causes the acceleration of a SN blast wave when it passes through and exits the dense envelope of a star (e.g., Matzner & McKee 1999). In general, a shock front will accelerate when it encounters a steeply falling density gradient (Gandel'man & Frank 1956; Sedov 1959; Sakurai 1960; Colgate & Johnson 1960; Imshennik & Nadězhin 1989; Ostriker & McKee 1988; Chevalier 1992). For a blast wave propagating through a medium with a density gradient given by $\rho \propto R^{-k}$, the velocity of a blast wave is described by

$$V_{BW} \propto R^{-\frac{(3-k)}{2}} \quad (3)$$

(see Ostriker & McKee 1988). For steady winds with $k=2$, the shock speed can be roughly constant or decelerate slowly, but for steeper density power laws of $k > 3$ the shock front will accelerate. Figure 5 shows a plausible density structure for the CSM around η Car, appropriate for our first model of an explosion running into a strong wind. Figure 5 shows a density that switches from the wind of η Car in its normal quiescent state before the eruption (presumably similar to its present day values of $\dot{M}=10^{-3} M_{\odot} \text{ yr}^{-1}$, $V_W = 500 \text{ km s}^{-1}$) to that of the assumed pre-eruption wind that produced the dense CSM needed for our favored model of CSM interaction ($\dot{M}=0.33 M_{\odot} \text{ yr}^{-1}$, $V_W = 200 \text{ km s}^{-1}$). If we assume a steady transition in \dot{M} that took place over a time period of an additional 30 yr preceding the dense wind, we get a slope of $k=7$ (shown in Figure 5). The density gradient could have been much steeper than this if the beginning of the eruption was more abrupt. Note that the drop in pre-shock density at this outer radius of the CSM is also a necessity for explaining the drop in luminosity at the end of the bright phase of the Great Eruption, and a steeper slope than shown in Figure 5 would be commensurate with the observed fading (but of course, there is also the possibility of dust formation or escape of radiation at shorter wavelengths as the material becomes more optically thin). The resulting change in

density is huge - roughly a factor of 10^4 over the change in radius Δr in Figure 5. For this conservative density power law of $k=7$, the scaling in equation (3) indicates that the blast wave would accelerate from 550 km s^{-1} at $R \simeq 3 \times 10^{16} \text{ cm}$ to more than $8,000 \text{ km s}^{-1}$ at $R \simeq 3 \times 10^{16} \text{ cm}$. For a steeper drop in density than this hypothetical example, the blast wave acceleration would be more severe.

The resulting very fast ejecta arise from rapid expansion of a relatively low mass ($\sim 0.1 M_\odot$; Smith 2008) of very hot gas located between the forward shock and the CDS, which supplies the pressure of the blast wave at the moment when it reaches the outer boundary of the dense CSM. During the most intense phase of CSM interaction (during the 10-15 yr after 1843), the forward shock would have been located immediately ahead of the CDS, as depicted in the left panel of Figure 4. The gas between the forward shock and the CDS is hot (10^6 - 10^7 K), but this zone is very thin. This is confirmed in numerical simulations of SNe IIn (van Marle et al. 2010). When the density of pre-shock CSM fell rapidly, the forward shock (which still contained $\sim 3 \times 10^{49}$ ergs of energy) would be free to expand. The resulting speed is likely to be highly latitude-dependent, of course. Acceleration of the forward shock in this way explains the absence of an obvious forward shock immediately ahead of the Homunculus, and the existence of the very rarefied cavity around the Homunculus at the present epoch. This acceleration of the forward shock essentially transfers the strong thermal pressure support of the blast wave into kinetic energy for a very small fraction of the total mass, thereby achieving speeds significantly larger than the original maximum speed of ejecta in the explosion. For a few 10^{49} ergs of energy in the forward shock, rough estimates are $V=5,000 \text{ km s}^{-1}$ and $0.1 M_\odot$.

Although the hot material immediately behind the forward shock will accelerate, most of the mass in the interaction was swept into the CDS and would continue to coast at the same speed when CSM interaction ends (the CDS does not accelerate because it is cold). Despite being compressed in a strong shock wave, the dense walls of the Homunculus are seen today as neutral or molecular gas and cool dust. This is because their extremely high densities allowed for very rapid and efficient cooling, which in turn powered the luminosity of the Great Eruption. The gas outside the Homunculus, however, is the result of a strong shock accelerating through much lower-density gas outside the pre-eruption CSM shell. This material was heated by the shock and was not able to cool efficiently, so it remains mostly ionized today. Smith (2008) estimated an average density of $n_e \simeq 500 \text{ cm}^{-3}$ for the fast ejecta outside the Homunculus; for this density, the recombination timescale

$$\tau = \frac{1}{n_e \alpha_B} \left(\frac{T}{10^4 \text{ K}} \right)^{0.8} \quad (4)$$

(where $\alpha_B = 2.6 \times 10^{-13} \text{ cm}^3 \text{ s}^{-1}$ is the hydrogen Case B recombination coefficient, and $T = 10^4 \text{ K}$ is the ionized gas temperature) is about 250 yr. Thus, the outer material heated by the forward shock would still be ionized, whereas the much denser material in the Homunculus would have long-since recombined. A strong shock passing through pre-existing dense clumps outside the Homunculus may provide a possible explanation for the origin of the long and thin whiskers/strings seen in *HST* images, but a satisfying explanation requires detailed numerical hydrodynamic simu-

lations outside the scope of this paper. It is likely that additional complications may be relevant in explaining the complex material outside the Homunculus, such as a reflected (reverse) shock resulting from the impact of the fast forward shock against the slower ejecta from a previous eruption.

3.8 What triggered the explosion?

By explaining this long list of observable peculiarities of η Car with this single simple CSM-interaction model adapted from SNe IIn, we distill the litany of many unsolved questions and inconsistencies down to one central mystery: *Why did Eta Car suffer a 10^{50} erg explosion in 1843/1844?* This question remains unsolved, since a $\sim 10^{50}$ erg explosion was assumed in our model. A number of potential physical mechanisms have been discussed (see, e.g., Smith et al. 2011 and references therein), including an explosion resulting from explosive burning of fresh fuel mixed into a shell burning layer. Perhaps this was triggered by a stellar collision, since the 1843 event coincided with a close periastron passage, although a collision alone supplies insufficient power (Smith 2011; Smith et al. 2011). A great deal of theoretical work on stellar interiors is needed before this is understood. Adopting a single explosion does, however, make the problem of η Car more tractable than having a large number of unrelated mysteries, if a physical explanation for such an explosion can be identified. Preliminary work does point to a tendency for very massive stars to undergo hydrodynamic eruptions/explosions (Young et al. 2005; Arnett, Meakin, & Young 2005).

4 IMPLICATIONS: EXTRAGALACTIC SUPERNOVA IMPOSTORS

Since η Car's Great Eruption occurred in the mid-19th century before modern optical spectrographs were available, and long before we were able to measure IR or X-ray radiation, we are limited to interpreting the historical visual light curve (Smith & Frew 2011). The fact that CSM interaction has long-since ended makes it difficult to test some of the predictions of a CSM-interaction model directly, which is why the Homunculus is such a valuable reservoir of physical information. This situation may soon change as we receive more valuable information about the spectrum of η Car's eruption through spectroscopy of its light echoes (Rest et al. 2012). In the mean time, however, we can also consider implications of the CSM-interaction scenario for transient sources that are thought to be extragalactic analogs of η Car.

Non-terminal eruptions or explosions that are analogous to η Car go by many names, including Type V supernovae, SN impostors, η Car analogs, intermediate luminosity optical/red transients, eruptive LBV-like transients, etc. (see Smith et al. 2011 and Van Dyk & Matheson 2012 for recent reviews).

If the CSM-interaction model is a viable interpretation of η Car's Great Eruption, it is likely that CSM interaction might play a role in some other extragalactic LBV-like transients as well. While some LBV-like transients exhibit the characteristic F-supergiant-like spectrum that one expects from a dense continuum-driven wind, a number of LBV-like eruptions do not fit that bill. There appear to

be two classes, identified as “hot LBVs” exemplified by the SN impostor SN 2009ip, and “cool LBVs” exemplified by UGC2773-OT (see Smith et al. 2011, 2010b). In particular, SN 2009ip showed optical spectra that closely resemble spectra of SNe IIn, with evidence for fast-moving ($1000\text{--}5000\text{ km s}^{-1}$) material seen only in absorption ahead of the photosphere (Smith et al. 2010b; Foley et al. 2011). This fast material might correspond to the fast blast wave seen in η Car’s ejecta. Like η Car, the light curve of SN 2009ip also showed a decade-long increase in brightness leading up to a brief eruption peak of -14 mag (Smith et al. 2010), and it has since re-brightened twice (Drake et al. 2010, 2012). Perhaps the initial decade-long brightening of SN 2009ip coincided with a strong wind that created a dense CSM, and the brief brightening was the explosive initiation of a shock wave, as in η Car. SN 2009ip is still under study, however. In any case, given the similarity between spectra of many LBV-like transients to those of SNe IIn, it is likely that CSM interaction may be quite widespread. Since the photosphere in many SNe IIn is located ahead of the forward shock in the very dense CSM, the same may be true for SN impostors if CSM interaction is important. If the emergent spectrum is formed in the pre-shock wind in some cases, it may be possible to determine the speeds of the pre-eruption wind and the expanding CDS from the time evolution of spectra, as is done for SNe IIn.

One important difference between η Car and other LBV-like transients is that most other SN impostors do not have high luminosities that last for a decade or more; η Car is quite unusual in this respect. In fact, most eruptive transients have typical durations of only 100 days (Smith et al. 2011), like the 1838 and 1843 events of η Car, but unlike its decade-long bright phase. We have argued that the long duration of high luminosity for η Car was caused by its explosion slowly overtaking very dense CSM, produced in a strong continuum-driven wind that blew for the preceding 30 years. This long wind phase may be relatively rare, since it is this phase that depends upon the star being extremely massive and luminous, near the classical Eddington limit. While $10^{49}\text{--}10^{50}$ erg explosions may occur over a wide range of initial masses (if, for example, the energy source is a deep-seated explosive shell burning event), perhaps the preceding super-Eddington wind phase - with sufficiently high mass-loss to make the CSM interaction last for a decade - is limited to the most massive stars like η Car. Lower-mass evolved stars may have dense and slow winds that produce opaque CSM as well, but the range of radii over which CSM densities are high-enough for efficient conversion of kinetic energy to visual light may be small. As a consequence, non-terminal explosive transients from lower-mass stars might tend to have shorter durations lacking prolonged CSM interaction, whereas the longer-duration events might be limited to more massive stars.

Although CSM interaction may be important in many of these transients, tracers of strong shocks like X-ray emission will not necessarily be detectable. In a SN IIn, much of the X-ray luminosity generated by the shock occurs in an optically thick region, and so the X-ray luminosity is reprocessed and escapes ultimately as visual-wavelength continuum radiation. This is why SNe IIn can be very luminous in the visual continuum. At late phases, when the forward shock outruns the outer boundary of the CSM shell and

accelerates, the X-rays may indeed escape, but the X-ray luminosity may be too faint to detect in most extragalactic transients. Likely the most fruitful avenue for searching for signs of CSM interaction is in detailed study of the visual-wavelength spectra of LBV-like transients.

5 SUMMARY

This paper has examined the hypothesis that the Great Eruption of η Carinae was powered by CSM interaction, where ejecta kinetic energy is converted to visual-wavelength luminosity in a radiative shock passing through dense CSM. By invoking an explosion of almost 10^{50} ergs occurring in 1843 that expands into dense CSM, the luminosity generated by CSM interaction provides an acceptable explanation for the 10-15 yr bright phase of the Great Eruption. We found that a CSM which is created by a slow 200 km s^{-1} wind with $\dot{M}=0.33 M_{\odot}\text{ yr}^{-1}$ provides a much better match to the historical light curve than CSM created by a previous explosion, although the parameters of the simple model can be adjusted somewhat. The wind needed to create the CSM is well-explained by existing models of continuum-driven super-Eddington winds (Owocki et al. 2004; van Marle et al. 2008, 2009), and the speed matches expectations for the star’s slower escape speed in the 1830s, based on its visual color and magnitude at that time. It also matches the observed wind speed seen in spectra of the 1890 eruption. Similarly, the physics of CSM interaction to explain the observed luminosity is taken from standard models for SNe IIn.

Borrowing again from models and observations of SNe IIn, we find that the CSM-interaction hypothesis can also explain a large number of previously perplexing observed properties of the Homunculus nebula. The most important consequence of CSM interaction is the creation of a cold dense shell (CDS) where most of the mass resides, which we identify with the thin walls of the massive Homunculus nebula. We find that the single scenario of CSM interaction gives a plausible explanation for (1) the ratio of kinetic energy of the Homunculus to the total radiated energy, (2) the double-shell structure of the Homunculus, with most of the mass in a thin outer shell containing cool dust and molecules, (3) the Hubble-like expansion of the Homunculus, (4) the bipolar shape of the Homunculus, with the caveat that published colliding-wind models need to be modified to limit the CSM interaction to a decade after the explosion with more mass and a highly radiative shock, (5) the efficient formation of dust grains in a thin shell, analogous to the rapid dust formation observed in SNe IIn and SNe Ibn, and (6) the acceleration of the forward shock upon reaching the outer boundary of the dense CSM, which leads to the very fast material in the outer ejecta and the soft X-ray shell around η Car. Each of these requires a different explanation, or mutually exclusive physical parameters in wind-only or explosion-only scenario for η Car, but they all arise naturally in the single model of CSM interaction.

Lastly, we speculate that the phenomenon of CSM interaction might be more widespread, and may play an important role in the physics and observed properties of a number of non-terminal LBV-like transients currently being discovered in external galaxies. Many of these non-SN transients may arise from weak ($10^{48}\text{--}10^{50}$ erg) explosions. Indeed,

some clear observational evidence supporting the presence of strong CSM interaction is already seen in some LBV-like transients. The presence of the same shock physics and observed consequences from CSM interaction further blur the distinction between true core-collapse SNe II_n and their non-terminal impostors, changing the framework in which we interpret LBV-like eruptions. This may make it more difficult to draw firm conclusions as to the underlying physical nature of any observed event (i.e. core collapse or non-terminal) based on the observed light curves and spectra, since both may be dominated by radiation from CSM interaction.

ACKNOWLEDGMENTS

I thank Stan Owocki for a number of thoughtful conversations about winds and LBV eruptions over the past decade, and for helpful comments on the manuscript. I also thank Dave Arnett for relevant discussions and helpful comments on the paper. Partial support was provided by the National Aeronautics and Space Administration (NASA) through grant AR-12618 from the Space Telescope Science Institute, which is operated by AURA, Inc., under NASA contract NAS5-26555. Based in part on observations obtained at the Gemini Observatory, which is operated by AURA, Inc., under a cooperative agreement with the NSF on behalf of the Gemini partnership: the National Science Foundation (USA), the Particle Physics and Astronomy Research Council (UK), the National Research Council (Canada), CONICYT (Chile), the Australian Research Council (Australia), CNPq (Brazil), and CONICET (Argentina).

REFERENCES

- Aerts, C., Lamers, H.J.G.L.M., & Molenberghs, G. 2004, *A&A*, 418, 639
- Arnett, D., Meakin, C., & Young, P.A. 2005, in *ASP Conf. Ser.* 332, *The Fate of the Most Massive Stars*, ed. R.M. Humphreys & K.Z. Stanek (San Francisco: ASP), 75
- Balbus, S.A., & Schaun, E. 2012, preprint (arXiv:1207.3810)
- Belyanin, A.A. 1999, *A&A*, 344, 199
- Castor, J.I., Abbott, D.C., & Klein, R.I. 1975, *ApJ*, 195, 157
- Chevalier, R.A. 1992, *ApJ*, 394, 599
- Chevalier, R.A., & Fransson, C. 1994, *ApJ*, 420, 268
- Chevalier, R.A., & Irwin, C.M. 2011, *ApJ*, 729, L6
- Chugai, N.N., & Danziger, I. J. 1994, *MNRAS*, 268, 173
- Chugai, N.N., et al. 2004, *MNRAS*, 352, 1213
- Clayton, D.D. 1979, *Ap&SS*, 65, 179
- Colgate, S.A., & Johnson, M.H. 1960, *Phys. Rev. Lett.*, 5, 235
- Corcoran, M.F., Rawley, G.L., Swank, J.H., & Petre, R. 1995, *ApJ*, 445, L121
- Corcoran, M.F., et al. 2004, *ApJ*, 613, 381
- Currie, D.G., et al. 1996, *AJ*, 112, 1115
- Crowther, P.A. 2007, *ARAA*, 45, 177
- Davidson, K. 1987, *ApJ*, 317, 760
- Davidson, K., & Humphreys, R.M. 1997, *ARAA*, 35, 1
- Davidson, K., Walborn, N.R., & Gull, T.R. 1982, *ApJ*, 254, L47
- Davidson, K., Dufour, R.J., Walborn, N.R., & Gull, T.R. et al. 1986, *ApJ*, 305, 867
- Dessart, L., Hillier, D.J., Gezari, S., Basa, S., & Matheson, T. 2009, *MNRAS*, 394, 21
- Drake, A.J., et al. 2010, *ATel*, 2897, 1
- Drake, A.J., et al. 2012, *ATel*, 4334, 1
- Duschl, W.J., Hofman, K.H., Rigaut, F., & Weigelt, G. 1995, in *The Eta Carinae Region*, ed. V. Niemala, N. Morrell, & A. Feinstein (*RevMexAA Ser. Conf.*, 2) (Mexico, D.F.: Inst. Astron. Univ. Nac. Autonoma Mexico), 17
- Dwarkadas, V., & Balick, B. 1998, *AJ*, 116, 829
- Dwarkadas, V., & Owocki, S.P. 2002, *ApJ*, 581, 1337
- Falk, S.W., & Arnett, W.D. 1977, *ApJS*, 33, 515
- Frank, A., & Mellema, G. 1994, *ApJ*, 430, 800
- Frank, A., Balick, B., & Davidson, K. 1995, *ApJ*, 441, L77
- Frank, A., Ryu, D., & Davidson, K. 1998, *ApJ*, 520, 291
- Fryxell, B., Müller, E., & Arnett, D. 1991, *ApJ*, 367, 619
- Foley, R.J., et al. 2011, *ApJ*, 732, 32
- Fox, O.D., et al. 2009, *ApJ*, 691, 650
- Fox, O.D., et al. 2011, *ApJ*, 741, 7
- Gallagher, J.S. 1989 in *IAU Coll. 113: Physics of Luminous Blue Variables*, ed. K. Davidson, A.F.J. Moffat, & H.J.G.L.M. Lamers (Dordrecht: Kluwer), 185
- Gandel'man, G.M., & Frank-Kamenetsky, D.A. 1956, *Sov. Phys. Dokl.*, 1, 223
- Gomez, H.L., Dunne, L., Eales, S.A., & Edmunds, M.G. 2006, *MNRAS*, 372, 1133
- Gomez, H.L., Vlahakis, C., Stretch, C.M., Dunne, L., Eales, S.A., Beelen, A., Gomez, E.L., & Edmunds, M.G. 2010, *MNRAS*, 401, L48
- Gonzalez, R.F., de Gouveia Dal Pino, E.M., Raga, A.C., & Velazquez, P.F. 2004, *ApJ*, 616, 976
- Gonzalez, R.F., Villa, A.M., Gomez, G.C., de Gouveia Dal Pino, E.M., Raga, A.C., Canto, J., Velazquez, P.F., & de la Fuente, E. 2010, *MNRAS*, 402, 1141
- Gull, T.R., Viera, G., Bruhweiler, F., Nielsen, K.E., Verner, E., & Danks, A. 2005, *ApJ*, 620, 442
- Hartman, H., Gull, T., Johansson, S., Smith, N., and HST Eta Carinae Treasury Project Team 2004, *A&A*, 419, 215
- Hillier, D.J., Davidson, K., Ishibashi, K., & Gull, T.R. 2001, *ApJ*, 553, 837
- Humphreys, R.M., Davidson, K., & Smith, N. 1999, *PASP*, 111, 1124
- Imshennik, V.S., & Nadëzhin, D.K. 1989, *Sov. Sci. Rev. E. Astrophys. Space Phys.*, 8, 1
- Joss, P.C., Salpeter, E.E., & Ostriker, J.P. 1973, *ApJ*, 181, 429
- Kankare, E., et al. 2012, *MNRAS*, 424, 855
- Kochanek, C.S. 2011, *ApJ*, 743, 73
- Kochanek, C.S. 2012, preprint (arXiv:1202.0281)
- Langer, N., Garcia-Segura, G., & Mac Low, M.M. 1999, *ApJ*, 520, L49
- Madura, T.I., Gull, T.R., Owocki, S.P., Groh, J.H., Okazaki, A.T., & Russell, C.M.P. 2012, *MNRAS*, 420, 2064
- Matzner, C.D., & McKee, C.F. 1999, *ApJ*, 510, 379
- Mauerhan, J., Smith, N., Silverman, J.M., Filippenko, A.V., Morgan, A. N., Cenko, S.B., Ganeshalingam, M., Clubb, K., & Matheson, T. 2012, preprint (arXiv:1209.0821)
- Mauerhan, J., & Smith, N. 2012, *MNRAS*, 424, 2659
- Meaburn, J., et al. 1996, *MNRAS*, 282, 1313
- Mellema, G., & Frank, A. 1995, *MNRAS*, 273, 401
- Meshkov, E.F. 1969, *Sov. Fluid Dyn.*, 4, 101
- Morse, J.A., Davidson, K., Bally, J., Ebbets, D., Balick, B., & Frank, A. 1998, 116, 2443
- Morse, J.A., Kellogg, J.R., Bally, J., Davidson, K., Balick, B., & Ebbets, D. 2001, *ApJ*, 548, L207
- Nielsen, K.E., Gull, T.R., & Veira-Kober, G. 2005, *ApJSS*, 157, 138
- Ofek, E.O., et al. 2007, *ApJ*, 659, L13
- Ostriker, J.P., & McKee, C.F. 1988, *Rev. Mod. Phys.*, 60, 1
- Owocki, S.P. 2003, *IAU Symp.* 212, *A Massive Star Odyssey*, ed. K. van der Hucht, A. Herrero, & C. Esteban (San Francisco: ASP), 281
- Owocki, S.P., Cranmer, S., & Gayley, K.G. 1996, *ApJ*, 472, L115
- Owocki, S.P., & Gayley, K.G. 1997, in *ASP Conf. Ser.* 120, *Luminous Blue Variables: Massive Stars in Transition*, ed. A. Nota & H. Lamwers (San Francisco: ASP), 121
- Owocki, S.P., Gayley, K.G., & Cranmer, S. 1998, in *ASP Conf.*

- Ser. 131, Boulder-Munich II: Properties of Hot, Luminous Stars, ed. I.D. Howarth (San Francisco: ASP), 237
- Owocki, S.P., Gayley, K.G., & Shaviv, N.J. 2004, *ApJ*, 616, 525
- Paczynski, B. 1990, *ApJ*, 363, 218
- Polonski, E., et al. 1999, *AJ*, 118, 2369
- Quinn, T., & Paczynski, B. 1985, *ApJ*, 289, 634
- Rest, A., et al. 2012, *Nature*, 482, 375
- Richtmyer, R.D. 1960, *Comm. on Pure and Appl. Math.*, 13, 297
- Roming, P.W.A., et al. 2012, *ApJ*, 751, 92
- Sakurai, A. 1960, *Comm. Pure Appl. Math.*, 13, 353
- Sedov, L.I. 1959, *Similarity and Dimensional Methods in Mechanics* (New York: Academic)
- Seward, F.D., Butt, Y.M., Karovska, M., Prestwich, A., Schlegel, E.M., & Corcoran, M.F. 2001, *ApJ*, 553, 832
- Shaviv, N.J. 2000, *ApJ*, 532, L137
- Shacham, T., & Shaviv, N.J. 2012, preprint (arXiv:1206.6078)
- Smith, N. 2002, *MNRAS*, 337, 1252
- Smith, N. 2006, *ApJ*, 644, 1151
- Smith, N. 2008, *Nature*, 455, 201
- Smith, N. 2009, arXiv:0906.2204
- Smith, N. 2010, *MNRAS*, 402, 145
- Smith, N. 2011, *MNRAS*, 415, 2020
- Smith, N., & Gehrz, R.D. 1998, *AJ*, 116, 823
- Smith, N., & Ferland, G.J. 2006, *ApJ*, 655, 911
- Smith, N., & Frew, D. 2011, *MNRAS*, 415, 2009
- Smith, N., & Mauerhan, J.C. 2012, *ATel*, 4412, 1
- Smith, N., & McCray, R. 2007, *ApJ*, 671, L17
- Smith, N., & Morse, J.A. 2004, *ApJ*, 605, 854
- Smith, N., & Owocki, S.P. 2006, *ApJ*, 645, L45
- Smith, N., & Townsend, R.H.D. 2007, *ApJ*, 666, 967
- Smith, N., Gehrz, R.D., & Krautter, J. 1998, *AJ*, 116, 1332
- Smith, N., Gehrz, R.D., Hinz, P.M., Hoffmann, W.F., Mamajek, E.E., & Meyer, M.R., & Hora, J.L. 2002, *ApJ*, 567, L77
- Smith, N., Gehrz, R.D., Hinz, P.M., Hoffmann, W.F., Hora, J.L., Mamajek, E.E., & Meyer, M.R. 2003b, *AJ*, 125, 1458
- Smith, N., et al. 2004, *ApJ*, 605, 405
- Smith, N., Morse, J.A., & Bally, J. 2005, *AJ*, 130, 1778
- Smith, N., et al. 2007, *ApJ*, 666, 1116
- Smith, N., et al. 2008a, *ApJ*, 686, 467
- Smith, N., Foley, R.J., & Filippenko, A.V. 2008b, *ApJ*, 680, 568
- Smith, N., et al. 2009, *ApJ*, 695, 1334
- Smith, N., Chornock, R., Silverman, J.M., Filippenko, A.V., & Foley, R.J. 2010, *ApJ*, 709, 856
- Smith, N., et al. 2010, *AJ*, 139, 1451
- Smith, N., Li, W., Silverman, J.M., Ganeshalingam, M., & Filippenko, A.V. 2011, *MNRAS*, 415, 773
- Smith, N., et al. 2012, *AJ*, 143, 17
- Soker, N. 2007, *ApJ*, 661, 490
- Van Dyk, S.D. 2005, in *ASP Conf. Ser. 332, The Fate of the Most Massive Stars*, ed. R.M. Humphreys & K.Z. Stanek (San Francisco: ASP), 47
- Van Dyk, S.D., & Matheson, T. 2012, in *Eta Carinae and the Supernova Impostors*, *ASSL* 384, 249
- van Marle, A.J., Owocki, S.P., Shaviv, N.J. 2008, *MNRAS*, 389, 1353
- van Marle, A.J., Owocki, S.P., Shaviv, N.J. 2009, *MNRAS*, 394, 595
- van Marle, A.J., Smith, N., Owocki, S.P., & van Veelen, B. 2010, *MNRAS*, 407, 2305
- Vishniac, E.T. 1994, *ApJ*, 428, 186
- Walborn, N.R. 1976, *ApJ*, 204, L17
- Walborn, N.R., & Liller, M. 1977, *ApJ*, 211, 181
- Walborn, N.R., & Blanco, B.M. 1988, *PASP*, 100, 797
- Walborn, N.R., Blanco, B.M., & Thackeray 1978, *ApJ*, 219, 498
- Weis, K., Duschl, W.J., & Chu, Y.H. 1999, *A&A*, 349, 467
- Weis, K. 2001, in *ASP Conf. Ser. 242, Eta Carinae and other Mysterious Stars*, ed. T. Gull, S. Johansson, & K. Davidson (San Francisco: ASP), 129
- Weis, K., Corcoran, M.F., Bomans, D.J., & Davidson, K. 2004, *A&A*, 415, 595
- Whitney, C.A. 1952, *Harvard Obs. Bull.*, 921, 8
- Woosley, S.P., Blinnikov, S., & Heger, A. 2007, *Nature*, 450, 390
- Young, P.A. 2005, in *ASP Conf. Ser. 332, The Fate of the Most Massive Stars*, ed. R.M. Humphreys & K.Z. Stanek (San Francisco: ASP), 190
- Zethson, T., Johansson, S., Davidson, K., Humphreys, R.M., Ishibashi, K., & Ebbets, D. 1999, *A&A*, 344, 211
- Zwicky, F. 1964, *ApJ*, 139, 514